PJET, Vol. 3, No. 2, July 2025: 30-50
Poly Journal of Engineering and Technology
j o u r n a l h o m e p a g e : https://journals.bdu.edu.et/index.php/PJET/index
ORGINAL ARTICLE

Performance analysis of solar photovoltaic panels integrated with PCMs and Fins

Muluken Z. Getie [a, *], Kassa E.Kasie [a, *], Hailemariam M. Wassie [a]

[a] Faculty of Mechanical and Industrial Engineering, Bahir Dar Institute of Technology, Bahir Dar University, Bahir Dar, P.O.Box: 26, Amhara, Ethiopia.

ABSTRACT

The design of cooling systems for solar PV panel systems has become increasingly important. The phase change materials, which are lower cost, have a long life, have reasonable efficiency, and can be integrated with different techniques, are a potential cooling mechanism for solar PV panels. In this study, numerical investigation and experimental testing of solar PV panels have been conducted using phase change materials (PCM) at different temperatures and fin arrangements. Transient numerical simulations were carried out with ANSYS Fluent software using a 2-D simplified geometry. Numerical simulations were used to evaluate the PV cell temperature and PCM thermal behavior. The numerical study was validated experimentally with PV-PT58/fins configured externally. The panel temperature was maintained below the reference panel temperature for the entire day by using PT58 and PT58/fins configured internally and externally. The average temperatures of the panel obtained from the numerical analysis were 32°C and 34.5°C for the experimental analysis, which are comparable. The experimental results show that the cooled PV module had an average efficiency of 12.03% compared to the uncooled panel's 10.84%, which is an improvement of 10.98% in the panel's electric efficiency.

Keywords: *Passive cooling, Numerical simulation, Experimental investigation, Solar Panel, Fins, PCM.*

DOI: https://doi.org/10.20372/pjet.v3i2.2706

Corresponding Author: Muluken Z. Getie
Faculty of Mechanical and Industrial Engineering, Bahir Dar Institute of Technology, Bahir Dar University, Bahir Dar, P.O.Box: 26, Amhara, Ethiopia
Email*:* muluken.zegeye@bdu.edu.et

Nomenclature

Symbol	Definition	Unit
AC	Alternative current	Ampere
Al	Aluminum	-
BIPV	Building integrated photovoltaic	-
Cu	Copper	-
CFD	Computational fluid dynamics	-
CIS	Copper indium selenide	-
DC	Direct current	Ampere
FC	Forced circulation	-
FF	Filler factor of the PV module	-
G	Solar radiation	W/m^2
h	Convection heat transfer coefficient	$W/K.m^2$
$\mathrm{I_{sc}}$	Short circuit current	Ampere
K	Thermal conductivity	$W/m.K$
L	Length	Meter
L_f	Latent heat	
NAC	Natural air circulation	-
OPCM	Organic phase change materials	-
PCM	Phase change materials	-
P_m	Electrical output power	Watt
PW	Paraffin wax	-
PV/T	Photovoltaic thermal	-
Q	Electron charge	C
ρ	Density	Kg/m^3
RET	Renewable energy target	-
RT	RubiTherm (PCM)	-
R_{th}	Thermal resistance	m^2K/W
PV	Photovoltaic	-
STC	Standard test condition	
T_{amb}	Ambient temperature	℃

TEG	Thermoelectric generator	-
TEM	Thermoelectric material/ module	-
TES	Thermal energy storage	-
η_c	Efficiency	%
V_{oc}	Open circuit voltage	Volt
α_{glass}	Absorptivity of glass	
β_{ref}	Temperature coefficient	K^{-1}

1. Introduction

The rapid industrialization, technological advancements, increasing energy consumption, and population growth contribute significantly to global warming and rising greenhouse gas emissions [1]. Renewable energy sources like wind, biomass, hydropower, and solar energy are crucial for addressing these challenges, with solar power being particularly attractive due to its availability, reliability, and versatility [2][3][4]. Efficient energy utilization is key to sustainable development, fostering a healthier society and improving productivity.

Despite the abundance of sunlight on Earth's surface, direct solar energy conversion remains inefficient, with only 10-20% of irradiation converted to electricity, while the rest is lost as heat [5]. Factors like photovoltaic (PV) panel material, solar radiation intensity, weather conditions, and geographical location affect PV panel performance. Research has shown that temperature and solar radiation significantly impact the performance of different types of solar cells, and efforts have been made to improve efficiency through various methods [6][7]. Cooling techniques such as fan-based and air-vent cooling, as well as phase change materials (PCMs) and nano-PCMs, have been explored to enhance the performance of PV systems [8][9][10][11]. These cooling methods have shown promising results in improving efficiency, but challenges such as optimal material selection and cooling system design remain [12].

Studies indicate that combining PCM and fins can significantly reduce the peak temperature of PV cells, thereby improving their efficiency [13][14]. New methods, like hybrid PV/T systems and microchannel cooling, continue to show potential for increasing energy output and efficiency [15][16][17]. Furthermore, research on PCM-based cooling solutions has shown financial and performance advantages, particularly in hot climates with high solar radiation [18]. The growing interest in solar energy utilization calls for further exploration of cooling techniques, particularly in adapting to varying climatic conditions, as geographical location significantly impacts solar energy performance.

In conclusion, while much has been done to enhance PV system performance using advanced cooling methods, ongoing research into optimizing PCM melting temperatures, fin designs, and the integration of cooling technologies across different climates is essential for the future of solar energy. This paper aims to contribute to the development of effective cooling techniques by exploring the integration of phase-change materials and fins for improving PV module performance.

2. Materials and Methods

2.1. Configuration and research flow

ANSYS Design Modeler 2022R1 created a 2D configuration that reflects the full layer of the proposed system. The PV panel contains six layers; including the glass cover, anti-reflective coating (ARC), PV cells, ethylene-vinyl acetate (EVA) layers, rear contact, and polyvinyl fluoride (Tedlar), as can be seen in Fig.1. Moreover, Fig. 1 demonstrates the typical PV-PCM configuration and the associated heat flow system. Each layer is individually designed and assembled based on its respective thickness and material properties. Various layers of the PV system listed earlier are considered during the numerical model, except for the ARC, due to its very small thickness. Externally configured fins are perforated through a 20-mm hole to account for the effect of wind speed. The dimensions & thermo-physical parameters of the components are presented in Table 1.

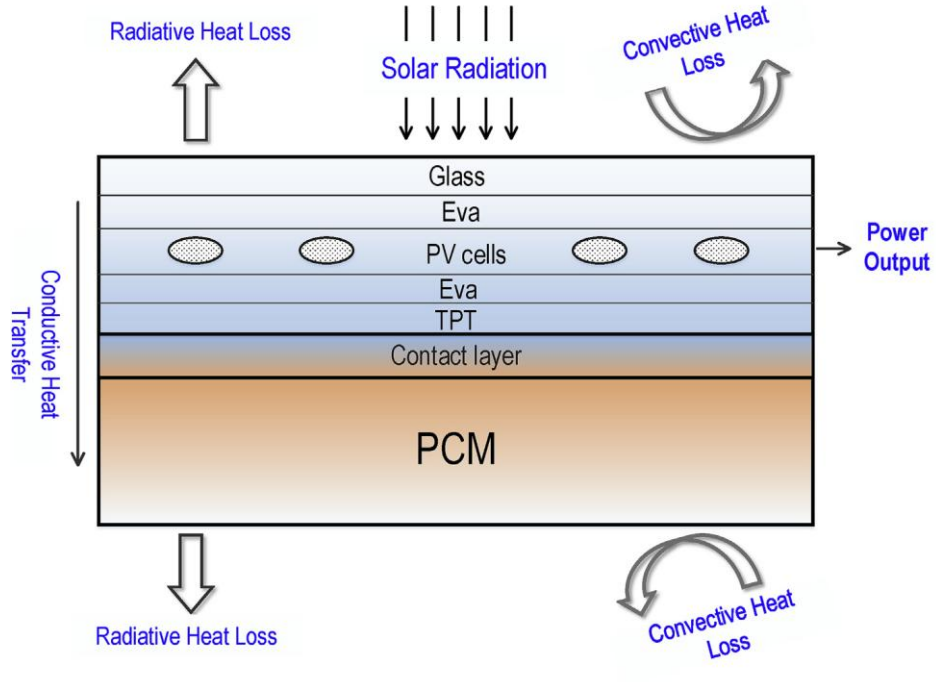

Fig. 1: The 2-D geometrical model of each layer of the PV panel

Table 1:Thermo-physical property of PV cell layers.

Layers	Thickness(mm)	K (W/mK)	ρ (Kg/m^3)	C_p (J/Kg.k)
Glass	3	1.8	3000	500
ARC	0.0001	32	2100	170
PV cell	0.3	148	2330	677
EVA	0.5	0.35	960	2090
Rear contact	0.2	237	2700	900
Tedlar	0.1	0.2	1200	1250
	Absorptivity	Reflectivity	Transmissivity	Emissivity
Glass	0.04	0.04	0.92	0.9

PV cell	0.9	0.08	0.02	
EVA	0.08	0.02	0.9	
Tedlar	0.13	0.86	0.012	0.9

The molten PCM was created and encapsulated in a 2-mm-thick aluminum container. Aluminum was selected because it is easily available and has a high thermal conductivity, which allows effective heat transfer between the PV and PCM. The physical model is presented in Fig. 2. Fig. 2 shows PV panels with PCM at different temperatures and with fins.

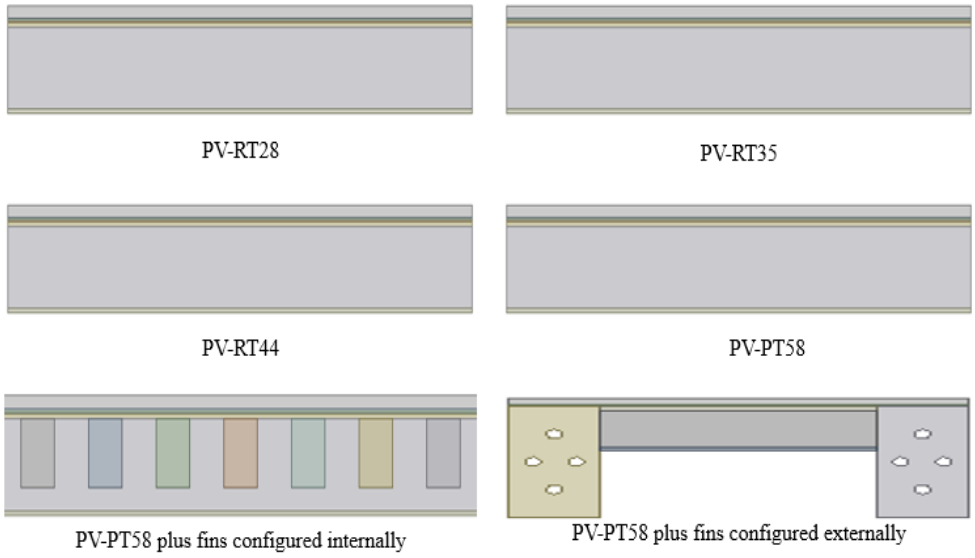

Fig. 2: Physical model for the developed system

The dimension of PCM was created and encapsulated in a 2-mm-thick aluminum container. Aluminium is selected because it is easily available and has a high thermal conductivity, which allows effective heat transfer to the PCM. As shown in Fig. 2, PV-PCM with a melting temperature of (28 ℃, 35℃, 44℃, and 58℃) and PT58/fins are configured both internally as well as externally. In the case of an external fin arrangement, perforated fins are used to account for the variation in wind speed. The thermophysical properties of PCMs are tabulated in Table 2.

Table 2: Properties of four PCMs [19], [20]–[22]

Properties	RT-28	RT-35	RT- 44	PT-58
Melting Temperature	27℃- 29℃	34℃-36℃	43 ℃-45℃	57 ℃-59℃
Congealing Temperature	29℃-27℃	36℃-34℃	45 ℃-43℃	59 ℃-57℃
Density of solid	880 Kg/m^3	880 Kg/m^3	800 Kg/m^3	890 Kg/m^3
Density of liquid	770 Kg/m^3	770 Kg/m^3	700 Kg/m^3	810 Kg/m^3
Specific heat capacity	2000 J/Kg.k	2000 J/Kg.k	2000 J/Kg.k	2410 J/Kg.k
Latent heat	250 kJ/Kg	240 KJ/Kg	250 KJ/Kg	225 KJ/Kg
Thermal conductivity	0.2 W/Mk	0.2 W/mK	0.23 W/mK	0.25 W/mK

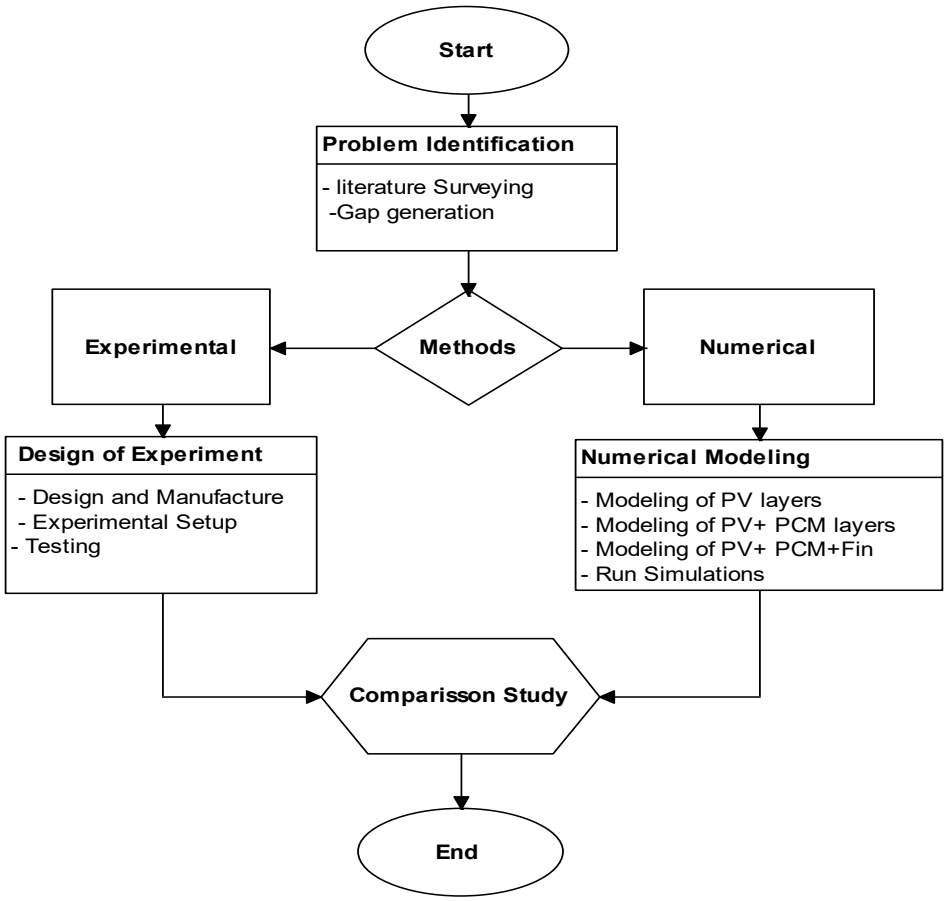

Fig. 3: General Research flow diagram

2.2. Mathematical modelling

The following assumptions are made while solving the numerical simulations:

- The incident radiation on the PV panel is uniform in all cases.
- The contact resistance between the different layers of the PV-PCM/fin system is negligible, and the sidewall heat losses are negligible.
- The thermal, mechanical, and physical properties of all components do not vary with temperature.
- The PV panel is clear without any agents of deposition or dust on the surface.
- The melted PCM in the liquid phase is assumed to be two-dimensional, incompressible, and Newtonian with unsteady flow and laminar flow.
- Conduction and convection modes are considered the dominant modes in the melted PCM.
- Subcooling of the PCM is not considered.
- PCM changes phase at a single constant temperature, which is the peak melting temperature where maximum energy is released and absorbed.

The numerical simulation is based on governing equations similar to the research conducted by [23],[24], [25]. Some of the governing equations of the numerical simulations are presented from equation (1)- (6).

Conservation of mass (Continuity equations) is evaluated by equation (1).

$$\partial \frac{(\rho u)}{\partial x} + \partial \frac{(\rho v)}{\partial y} = 0 \quad (1)$$

The general momentum equation is computed using equation (2).

$$\rho\left[\frac{\partial V}{\partial t} + \left(\vec{V} \nabla \vec{V}\right)\right] = -\nabla p + \nabla\left(\mu \nabla \vec{V}\right) + s \quad (2)$$

Energy conservation is determined by equation (3) as follows:

$$\frac{\partial}{\partial t}\left(\rho C_p T\right) + \frac{\partial}{\partial x}\left(\rho C_p u T\right) + \frac{\partial}{\partial y}\left(\rho C_p v T\right) = \frac{\partial}{\partial x}\left(k \frac{\partial T}{\partial x}\right) + \frac{\partial}{\partial y}\left(k \frac{\partial T}{\partial y}\right) - S_T \quad (3)$$

where

$$S_T = \frac{\partial}{\partial t}(\rho \Delta H) + \frac{\partial}{\partial x}(\rho U \Delta H) + \frac{\partial}{\partial y}(\rho V \Delta H) \quad (4)$$

Where ρ is the density of the fluid (kg/m^3); u and v are the x and y velocity (m/s) respectively; g is the acceleration due to gravity$(kg\ m/s^2)$.

2.3. Phase change material modeling

The temperature-dependent properties of phase change materials can be modeled using functions such as β, which is defined in equation (5). The function of β is expressed as which is the latent heat of the material.

$$\beta = \begin{Bmatrix} 0 \\ \frac{T - T_{solid}}{T_{liquid} - T_{solid}} \\ 1 \end{Bmatrix} \begin{Bmatrix} if\ T \le T_{solid} \\ if\ T_{solid} \le T \le T_{liquid} \\ T \ge T_{liquid} \end{Bmatrix} \quad (5)$$

The thermal behavior of the PCM is computed by the liquid fraction of the PCM. The liquid fraction shows whether the phase change material is solid, liquid, and in the mushy region. It is defined using equation (6).

$$LF = \begin{Bmatrix} 0 & T_{PCM} < T_m\ Solid\ phase \\ 1 & T_{PCM} > T_m liquid\ phase \end{Bmatrix} \quad (6)$$

Procedure of numerical investigation

ANSYS Fluent 2022 R1 uses the finite volume technique (FVM) to solve the transient governing equations. PV-PCM and PV-PCM/Fin geometries are created, and the "cell zone" conditions of the CFD package are employed to carry out the material assigned to the constituents. To perform the thermal-fluid simulations, the heat transfer in solids (panel, aluminum, solid-state PCM, and Fin) is coupled with heat transfer in fluids (liquid PCM) by invoking laminar flow in fluids. This enables the numerical simulation of conduction heat transfer in solid domains as well as natural convection within the liquid PCM. Specifically, the PCM is modeled as a fluid, and the solidification and melting model through the Boussinesq approximation implements its dual phase change response to temperature changes. Transient boundary conditions in tabular form were used to define the solar irradiance. The velocity and pressure fields are coupled using the SIMPLE method. The pressure correction equations were resolved using the PRESTO! Technique. Using the second-order upwind technique, the convective terms of the momentum and energy equations were discretized. The density, pressure, and momentum under-relaxation factors were 1.0, 0.3, and 0.2, respectively. A time step of 1S and 20 maximum iterations for 25,200 flow times were used for the simulations. At each time step, the numerical residuals were tested, with a convergence criterion of 10^{-6} applied for continuity and momentum and 10^{-9} for conservation of energy.

3. Experimental Testing and Validation

3.1. Preparation

At the start of the process, the PCM was solid. It was melted on a heat plate before being poured into the provided container (detailed dimensions are provided in Table *3*). The PCM is then placed into a 25 mm deep aluminum container after it has melted. To consider the change in volume during melting, 10% of the 25 mm depth of the container was spaced free. The preparation procedure and a 3D view of the fabricated prototype are shown in Fig. 4 and Fig. 5, respectively.

Table 3:The dimensions of the PCM container.

Parameters	Quantitative description
Material type	Aluminum
Length	300 mm
Depth (thickness)	25 mm
Width	130 mm
Numbers of Container	3

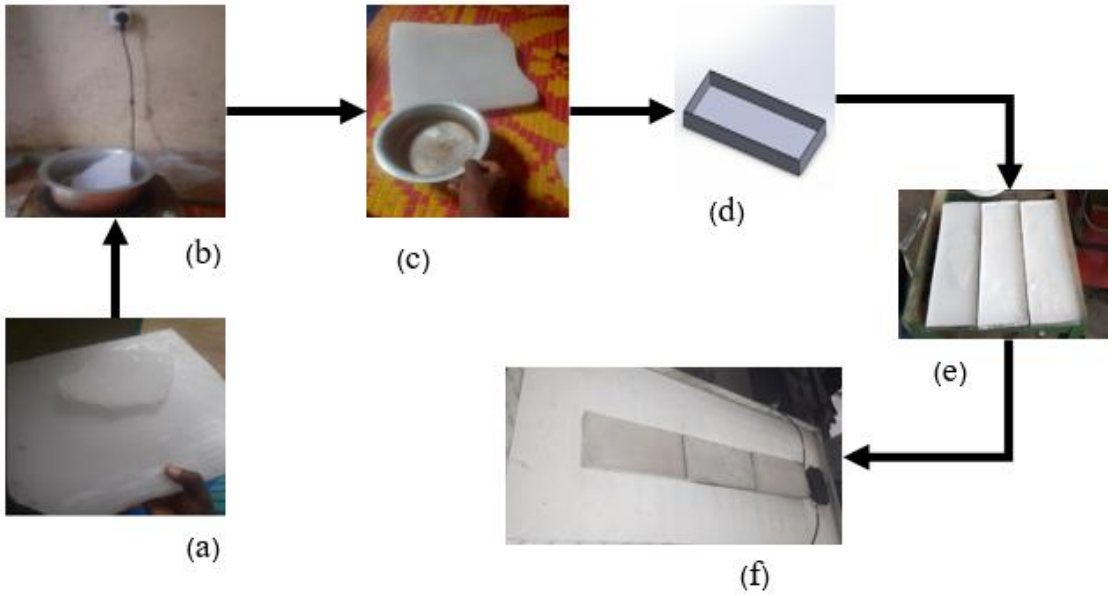

Fig. 4: schematic diagram for the preparation procedure of PCM. (a), solid PCM. (b), melting PCM. (c), liquid form of PCM. (e), pouring molten PCM in to Al container. (f), mounting PCM on the rear side of the PV panel.

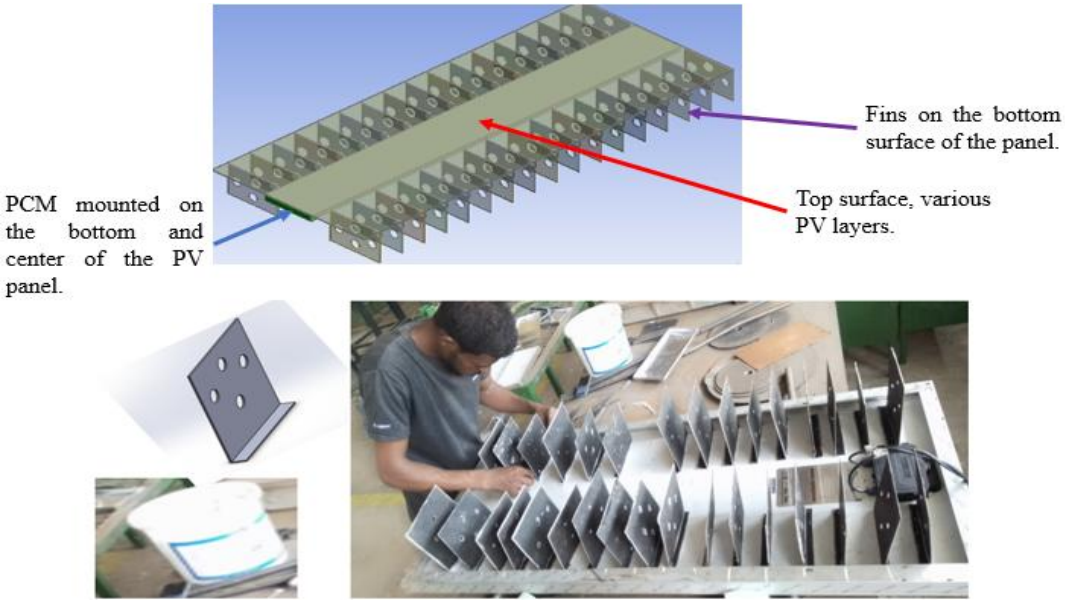

Fig. 5: Photograph and 3-D view of the prototype.

3.2. Set up

The whole experimental setup has been installed in Bahir Dar, Ethiopia, at a latitude of 11° 35' 59.99"N and a longitude of 37° 22' 59.99"E. In the experiment, two solar panels with similar maximum power ratings of 100W were employed. For comparison, one is free, whereas the other has a PCM and perforated fins on the rear side of the PV module as shown in Fig. 6. The 2 mm of aluminum sheet thickness sealed and shielded the PCM. The two panels are placed on

the stand relatively close to one another so that the sun's radiation incident on both panels is nearly equal to obtain equal amounts of solar energy.

The experiment was conducted for a week, from June 8 to June 20, 2022. The major components of the system are the PV panel, PCM, fins, and measurement tools, like pyranometers, clamp meters, and thermocouples. The variables that were measured throughout the experiment were recorded by averaging the data including the PV panel surface temperature, ambient temperature, solar radiation, load current, and load voltage.

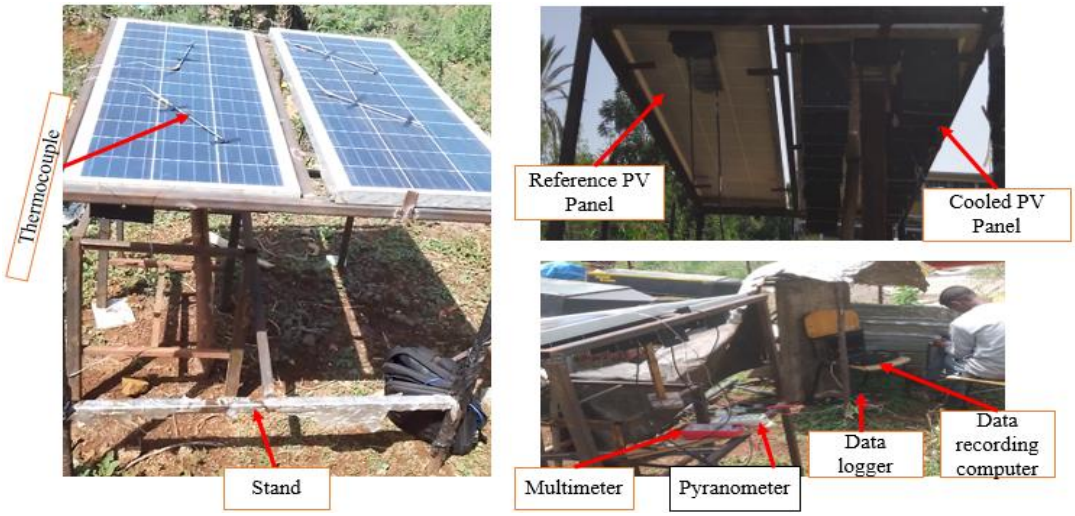

Fig. 6: Experimental set up

3.3.Test procedure

The measuring equipment was correctly set up on the experiment's rig. A pyranometer was placed between the two panels. The panel's front and back surface temperatures were monitored using six thermocouples. Four thermocouples were used to measure the front surface temperature of the PV module; two for reference and two for the cooled panel. Two thermocouples were used to measure the rear side temperature of the PV panel; one for the reference panel and the other for the cooled panel. The ambient temperature at the location was measured using one thermocouple. The voltage and current of both panels were measured every 20 minutes, which took an average of an hour. All measuring tools used for these investigations were pre-validated and tested for accuracy within the recommended range.

The performance of the PV panel is determined by its electrical power output. The electrical output power (P_m) of the PV system is influenced by the fluctuation in the PV panel temperature and is determined for the respective current (I_m) and voltage (V_m) using equation (7) as stated in [26]:

$$P_m = I_m V_m \tag{7}$$

Another parameter that must be considered when evaluating the performance of PV modules is the fill factor (FF). The fill factor is the ratio of the actual maximum power to the short-circuit current (I_{sc}) and the open circuit voltage (V_{oc}). The fill factor measures the effectiveness of a PV module, and it varies based on the elements or materials as provided in equation (8).

$$FF = \frac{P_m}{I_{sc} V_{oc}} \tag{8}$$

After obtaining the PV module's temperature, during the experimental period, the electrical efficiency of the PV module was estimated using the Evans and Florschuetz equation [37] as shown in equation (9).

$$\dot{\eta} = \dot{\eta}_{ref}\left[1 - \beta_{ref}(T_c - T_r)\right] \quad (9)$$

Where the actual temperature of the panel is denoted by T_c the efficiency of the panel under the standard test condition is denoted by $\dot{\eta}_{ref}$, and the reference temperature T_r is the ambient temperature. The temperature coefficient (β_{ref}) used for this study is taken as $0.004K^{-1}$ [19]. The electrical efficiency improvement for the PV module is determined using equation (10) [27].

$$improvement = \frac{\dot{\eta}_{cooled\ PV} - \dot{\eta}_{ref\ PV}}{\dot{\eta}_{ref\ PV}} \times 100\% \quad (10)$$

3.4.Validation

In this section, a comparison was made between the numerical and experimental results, as well as a comparison with earlier studies. In the case of the cooled panel, the maximum temperature recorded using the numerical simulation was 32.5℃ compared to the 33.6℃ recorded using the experimental taste. Table 4 illustrates that the percentage error for temperature between the numerical and experimental investigations varies between -0.7% to 8.5%, which is a tolerable deviation. Hence, the model is valid to design a solar PV cooling system.

Table 4: PV panel temperature for numerical and experimental investigation

Time (hr.)	**9:30**	**10:30**	**11:30**	**12:30**	**13:30**	**14:30**	**15:30**
Surface Temp. (Numerical)	30.73	31.13	30.66	30.73	32.31	32.5	32.67
Surface Temp. (Experiment)	30.53	31.4	32.7	33.6	33.8	33.6	32.7
% of error	-0.7	0.9	6.2	8.5	4.4	3.3	0.1

These differences could be explained by the fact that the wind speed was assumed to be constant in the case of the numerical simulation, whereas the experimental record was more accurate than that of the numerical simulation. The numerical simulation illustrated that the cooled panels had a relatively uniform temperature distribution, which was due to the cooling medium placed uniformly behind the panel. Validation was conducted using phase change material at PV-PT58/fins configured externally.

4. Result and discussion

4.1. PCM and PV panel temperature

This work presents investigations of the performance of thermal energy storage systems with six different melting point PCMs and a PV panel without PCM. The evaluation involving investigation of average temperatures of each PCM types (RT28, RT35, RT44, PT58, and PT58/fins configured internally and externally) and PV panel surface temperature without PCM are presented in Fig.7. As demonstrated in the figure, the temperatures of RT-28 and RT-35 PCMs are lower than the panel temperature at the beginning of the day nearly until 48 and 160 minutes,

respectively. Moreover, it has been seen that sensible heating and latent heating for RT-28 PCM happen relatively quickly. Both PCMs' temperatures significantly increased over the panel temperature following the indicated time. This implies that low melting point PCMs could function well at lower temperature ranges or low climate temperatures. This is very similar to the advice made by [28], who revealed that low meting point PCMs ought not to be utilized in areas with high ambient temperatures. Using PCMS with a low melting point temperature result in a cooled panel with a greater surface temperature than the reference panel. The usage of PCM will have a negative impact on PV system efficiency when the cell temperature is not higher than the PCM's melting point. This is due to the PCM's rapid melting and transition into liquid, which releases heat to the panel's back side which is confirmed by [29]. The temperatures of PCMs for R-44, PT58 and PT58/fins are significantly lower than the panel temperature, indicating that this configuration may be able to absorb and store more heat before completely melted. After about 386 minutes, only the temperature of the RT-44 surpasses the panel temperature. The temperatures of all of the PT58 arrangements', nevertheless, exhibit small temperature variation. For instance, the temperature of PT58/fins with external configuration raise from 300 K to 307 K.

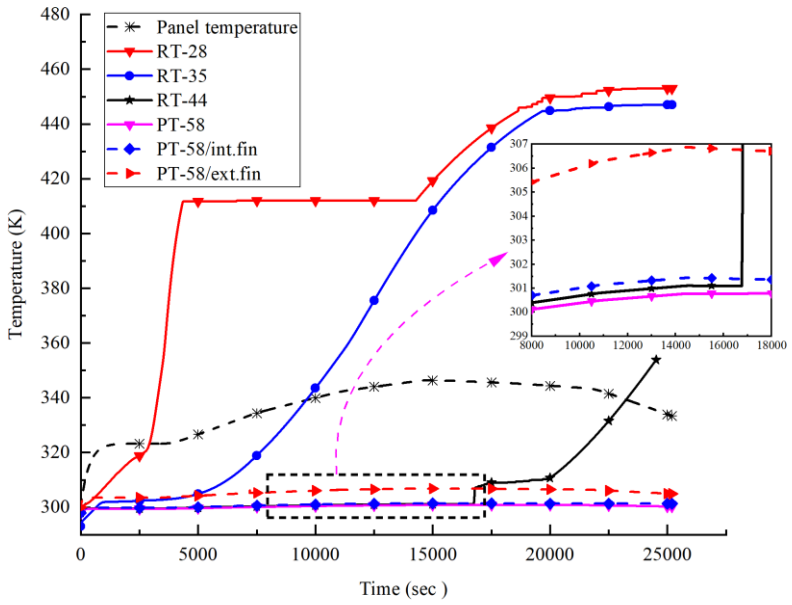

Fig. 7: Temperature profile of the numerical simulation of the solar PV panel

4.2. Liquid fraction analysis of PCM

The thermal behaviour of the PCM was investigated using a liquid fraction. The liquid fraction (LF) of the PCM, computed numerically, is presented in Fig. 8. Fig. 8 reveals that the lower the melting temperature of the PCM, the faster the phase shift from solid to liquid by absorbing more heat. For PV-RT28, PV-RT35, and PV-RT44 LF shifted from the zero (solid) phase to the one (liquid) phase after 2 h (1000 s), 3:30 h (10900 s) and 4:50 h (17400 s), respectively. The low melting point PCM starts melting and fully converted to liquid early. How ever, the rate of melting for PV-RT28, PV-RT35, and PV-RT44 are similar. On the other hand, LF is kept zero for all with and without fin arrangements of PV-PT58, demonstrating that such PCMs are fully in solid state and still could absorb

more heat energy. Therefore, there could an effective enhancement in the efficiency of the PV module owing to the use of the PV-PT58 with fins configured internally and externally.

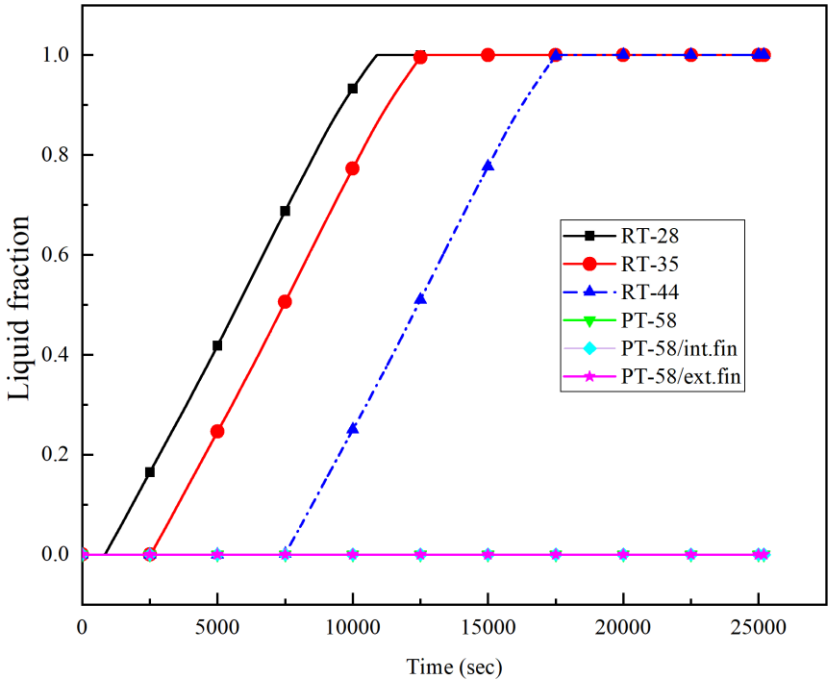

Fig. 8: Liquid Fraction analysis of PCM

4.3.Surface Temperature of PV Panels

The surface temperatures of the two modules were determined by averaging the surface temperatures measured by each of the six thermocouples placed on the upper and bottom surfaces of the panels. Fig. 9 shows the results for the temperature distributions of the experiment. As shown in Fig. 9, the surface temperature of the reference panel reached its peak between 11:30 and 13:30. This is due to the high level of solar radiation and ambient temperature observed at that time. However, owing to the efficiency of the cooling system, the cooled panel was able to keep its temperature relatively stable. However, at 13:30, the cooled panel-surface temperature began to decline because of a precipitous decrease in both solar radiation and ambient temperature. According to the results, the cooled system recorded an average temperature of 32°C while the uncooled system recorded an average temperature of 52.8°C. The average temperature difference between the reference and cooled panels is 20.8°C. The temperature improvements resulting from the cooling mechanisms were determined, as shown in Fig. 10. The maximum temperature improvement of the cooled PV panel was achieved at midday, which is about 26℃, which is higher than the similar study reported [30], as the maximum temperature was reduced by 13.5 ºC using 11 fins.

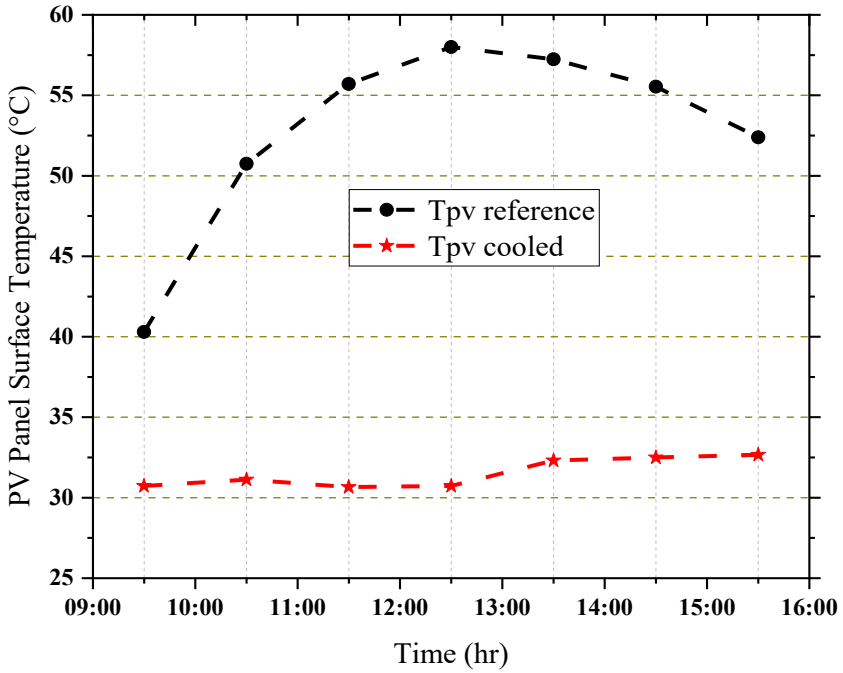

Fig. 9: Temperature distribution of the reference and cooled panels

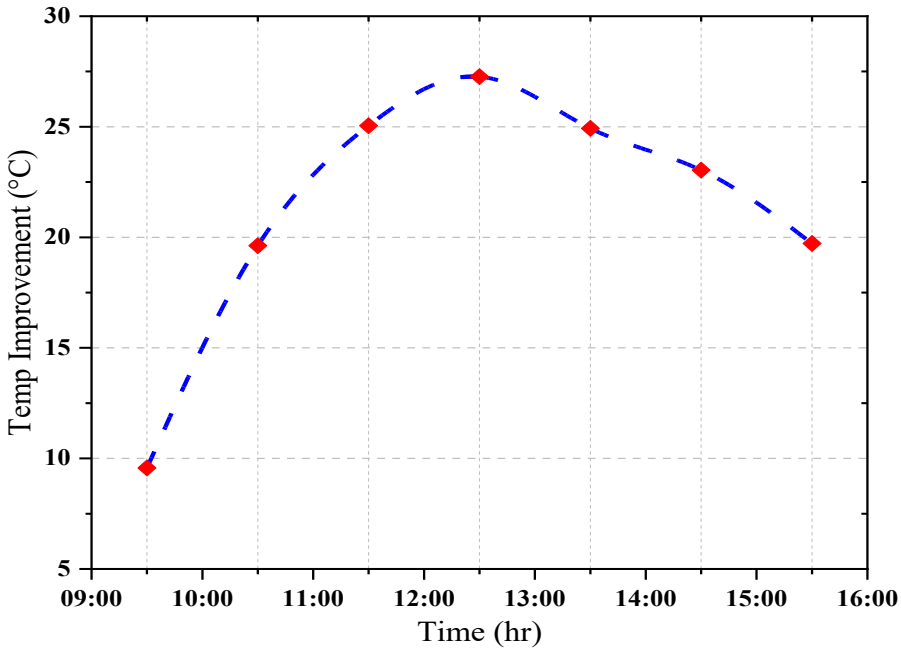

Fig. 10: Change in Temperature between reference and cooled panels.

In other cooling mechanisms, such as in [31], which employed a hybrid cooling mechanism of active using water and passive using a fin heat sink, the researchers obtained a 23.55℃ temperature drop, 30.3% improvements in the output power, and 11.9% improvements in electrical efficiency. The authors of [32], proposed a passive cooling method using a PCM with a melting temperature of 38-40℃. The panel temperature was improved by 15℃ in comparison to the single panel without PCM. In [27], they assessed experimentally the electrical and thermal characteristics of a PV

module cooled using fins and an ultrasonic humidifier. Their results showed that the cooling process in the study was able to reduce the temperature of the panel by an average of 14.61℃; hence, the current study has a relatively superior result.

4.4. Power Output and Electrical Efficiency Analysis

The electrical power outputs of the reference and cooled photovoltaic panels are shown in Fig. 11. Fig. 11 shows that, the power of the cooled and reference panels at the beginning and end of the test were nearly equal. However, as the surface temperature increased in response to the rising solar radiation, the reference panel's output power decreased and the power of the cooled panel increased. Compared with the reference panel, the power production from the cooled panel remained higher throughout the test. A maximum power output of 91.66W has been found using a cooled PV panel as compared to a maximum of 80.64W power in the reference panel. Hence, a 13.7% enhancement in power output was found using PV cooling in this study which is higher than the similar study conducted by [42], which reported power enhancements of 5.23% and 13.3% (1-PCM) by [30].

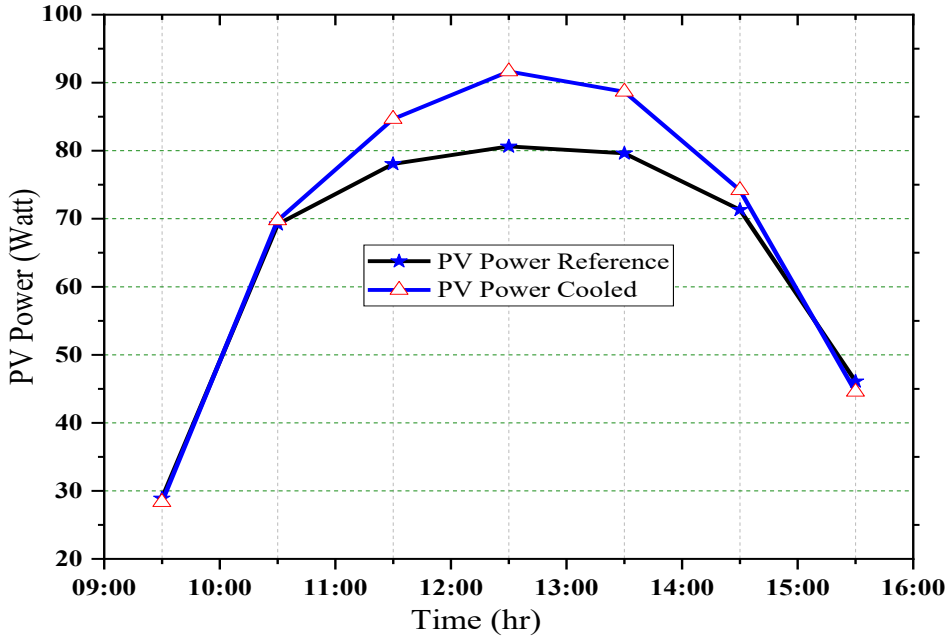

Fig. 11: Electrical power output compression of the Two PV panel.

Fig. 12 shows the electrical efficiencies of the two PV panels. The experimental findings show that the cooled PV panel had an average efficiency of 12.03% compared to the uncooled panel's 10.84%. A 10.98% improvement in electrical efficiency has been found using the cooled panel. The maximum efficiencies of the cooled and non-cooled PV panels have been found as 13.1% and 11.79 %. This resulted in a 10% efficiency improvement, which is much higher than that reported in a similar study conducted by [33].

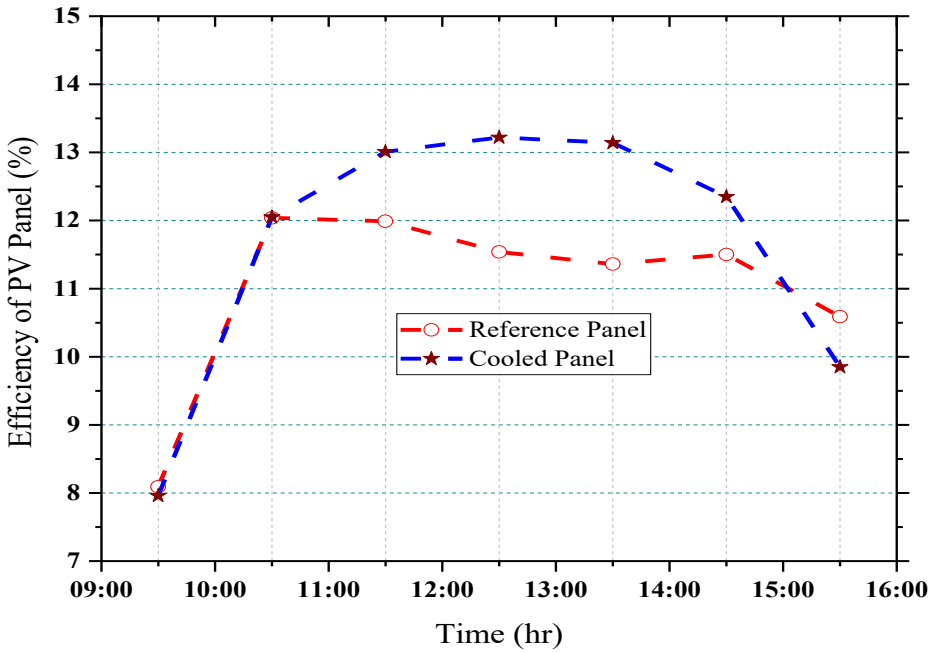

Fig. 12: Electrical efficiency compression of the reference and cooled panels.

The efficiency of the panel decreases sharply after midday, when the temperature of the panel is at its highest. The negative improvement recorded at the beginning and end of the experiment indicates that the uncooled panel was more efficient at the time of the experiment. This is because the heat stored by the PCM decreased the efficiency of the cooled panel. Moreover, the cooled panel was deficient in natural air at the rear side of the panel during that period because both the PCM and the fins were at its back. As a result, the uncooled panel was cooled by the ambient air at the start, and at the end of the experiment was relatively colder. Similar investigations are concluded in other cooling mechanisms such as [31] using water for the front surface and cotton wick mesh for the back surface. However, as soon as the cooling process started, the efficiency of the cooled panel significantly increased. This suggests that the method for cooling the PV panel is efficient. The efficiency improvement due to the cooling system is presented in Fig. 13. Fig. 13 demonstrates that the efficiency improvement is increased near to the midday, when the ambient temperature is at its maximum.

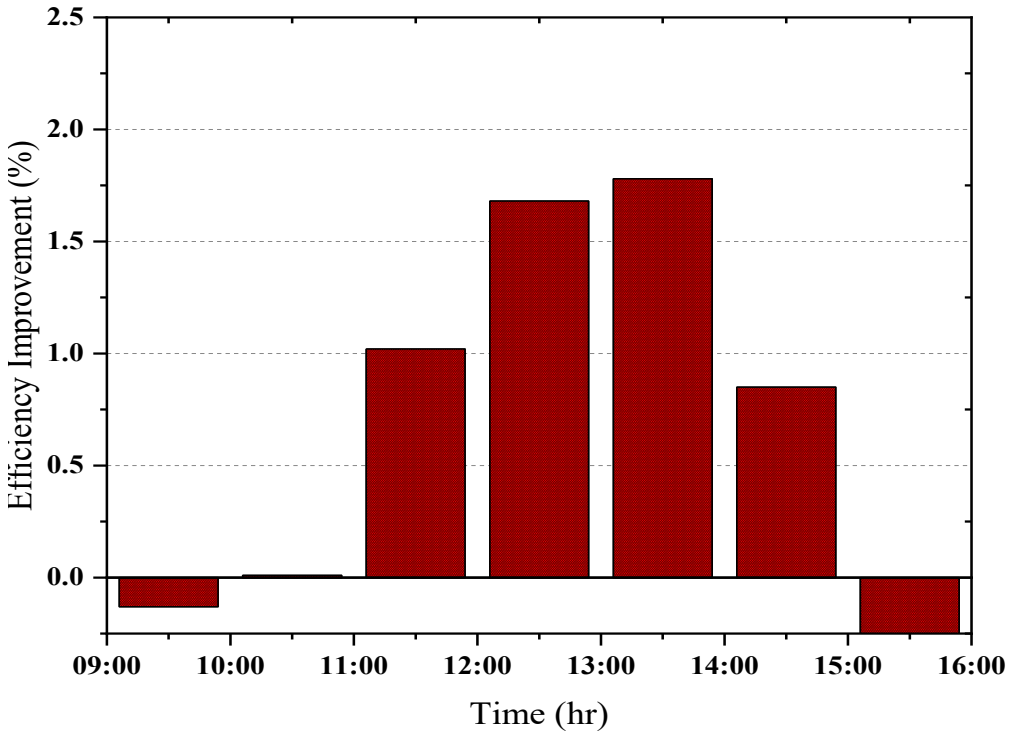

Fig. 13: Efficiency Improvement of the cooled PV panel.

4.5.Model Comparison

To validate and investigate the viability of the current study, it would be advisable to compare the current model with similar researches. The current study has been compared with the research findings from the literature and presented in Table 5. Such a comparison illustrates that this research is worth investigating.

Table 5: The comparison results of various cooling methods and the current study.

Reference	Cooling medium	Cooling methods	Temperature improvement	Efficiency improvement
[34]	PT58 PCM, PT58 PCM plus 8mm thick foam, PT58 PCM plus 12 mm thick foam.	Passive	3.33℃, 6.9℃, and 9.03℃ respectively	11.32%, 11.50%,and 11.77% respectively
	RT44, RT 44 plus PCM having 8mm thick foam, and RT 44 plus PCM having 12mm foam	Passive	11.25℃, 20.95℃, and 24.39℃ respectively	11.68%,11.79%, and 12.06% respectively
[35]	Dual surface cooling of PV panel. The front surface was cooled by water and the rear surface was using cotton wick mesh.	Passive	Surface temperature drop by 23.55℃ due to dual surface cooling.	11.9% improvement in electrical efficiency.

[36]	PT 58/ nano particles. The nanoparticles used were: multiwall carbon nanoparticles, Graphene, and Magnesium Nanoparticles with 0.25wt% and 0.5wt%.	Active	The maximum temperature improvement was obtained using graphene nanoparticles. 6.53℃ and 9.94℃ respectively for 0.25wt% and 0.5wt%.	Electrical efficiency was improved by 11.97%, and 12.10% respectively.
[37]	Conducted experimentally using Paraffin, sheep fat, and sheep fat plus CuO.	Active	The temperature improvement was 10℃, 15℃, and 20℃ for paraffin, sheep fat, and sheep fat plus CuO respectively.	The electrical improvement was 8.5%, 10.26%, and 12%.
[16]	Using a solar PV/T-PCM-TEG hybrid system; RT55 paraffin wax and placing copper fins around the copper	Active	Power output improved by 14.22% from the base standard PV panel power output.	increased from 30% to 35.2%
Current study	PV- PCM (RT28, RT35, RT44), PV-PT58, and PV-PT58 + Fins configured internally and externally.	Passive	The experiment was conducted with PT58 plus fins configured externally.	The electrical efficiency improvement was 10.98%

5. Conclusion

This study presents both numerical and experimental analyses of a passive cooling approach using four organic phase change materials (PCMs)—RT28, RT35, RT44, and PT58—integrated with fins (PV-PT58 + Fins) for temperature management of solar photovoltaic (PV) panels.

Key findings from the study are as follows:

- The numerical analysis demonstrated that the temperature of PV panels with RT28, RT35, and RT44 remained effectively managed for 1, 2, and 3 hours, respectively.
- Thermal behavior analysis of higher-melting temperature PCMs, such as PV-PT58 integrated with fins, indicated that the material stayed in its solid state (liquid fraction = 0%), resulting in improved performance, especially when combined with fins.
- The average panel temperatures from numerical simulations were 32°C, while the experimental study recorded an average of 34.5°C, showing close agreement between the two methods.
- Experimental results indicated that the cooled PV module achieved an average efficiency of 12.03%, compared to 10.84% for the uncooled panel.

For future research, the following enhancements are recommended:

- A comprehensive melting-solidification model using computational fluid dynamics (CFD) should be applied to better understand the thermal behavior of PCM and fin configurations.
- Further studies should evaluate the economic and environmental feasibility of different PCMs to assess their practicality for large-scale applications.

Funding

No funding was received for this research

Declaration of competing interest

The authors declare that they have no known competing financial interests or personal relationships that could have appeared to influence the work reported in this paper.

Data availability statement: Data available on request from the authors

Author contribution: ***Muluken Z.Getie:*** Conceptualization, methodology, validation, data curation, supervision, reviewing and final manuscript editing; ***Kassa E.Kasie***: Conceptualization, methodology, software, experiment, analysis, and initial draft; ***Hailemariam M.Wassie***; Software, experiment, Validation, and writing original draft, all authors have read and agreed to the published version of the manuscript.

4. Reference

[1] S. K. Marudaipillai, B. Karuppudayar Ramaraj, R. K. Kottala, and M. Lakshmanan, "Experimental study on thermal management and performance improvement of solar PV panel cooling using form stable phase change material," *Energy Sources, Part A Recover. Util. Environ. Eff.*, vol. 45, no. 1, pp. 160–177, 2023, doi: 10.1080/15567036.2020.1806409.

[2] S. Ni, "A novel and effective passive cooling strategy for photovoltaic panel," vol. 145, no. April, 2021, doi: 10.1016/j.rser.2021.111164.

[3] S. Verma, S. Mohapatra, S. Chowdhury, and G. Dwivedi, "Cooling techniques of the PV module: A review," *Mater. Today Proc.*, vol. 38, no. xxxx, pp. 253–258, 2020, doi: 10.1016/j.matpr.2020.07.130.

[4] M. S. Yousef, M. Sharaf, and A. S. Huzayyin, "Energy , exergy , economic , and enviroeconomic assessment of a photovoltaic module incorporated with a paraf fi n-metal foam composite : An experimental study," *Energy*, vol. 238, p. 121807, 2022, doi: 10.1016/j.energy.2021.121807.

[5] A. E. Kabeel, M. Abdelgaied, and R. Sathyamurthy, "A comprehensive investigation of the optimization cooling technique for improving the performance of PV module with reflectors under Egyptian conditions," *Sol. Energy*, vol. 186, no. May, pp. 257–263, 2019, doi: 10.1016/j.solener.2019.05.019.

[6] D. T. Cotfas, P. A. Cotfas, and O. M. Machidon, "Study of temperature coefficients for parameters of photovoltaic cells," *Int. J. Photoenergy*, vol. 2018, 2018, doi: 10.1155/2018/5945602.

[7] J. Adeeb, A. Farhan, and A. Al-Salaymeh, "Temperature effect on performance of different solar cell technologies," *J. Ecol. Eng.*, vol. 20, no. 5, pp. 249–254, 2019, doi: 10.12911/22998993/105543.

[8] Z. Syafiqah, N. A. M. Amin, Y. M. Irwan, M. S. A. Majid, and N. A. Aziz, "Simulation study of air and water cooled photovoltaic panel using ANSYS," *J. Phys. Conf. Ser.*, vol. 908, no. 1, 2017, doi: 10.1088/1742-6596/908/1/012074.

[9] A. R. Amelia *et al.*, "Cooling on photovoltaic panel using forced air convection induced by DC fan," *Int. J. Electr. Comput. Eng.*, vol. 6, no. 2, pp. 526–534, 2016, doi: 10.11591/ijece.v6i1.9118.

10] U. Sajjad, M. Amer, H. M. Ali, A. Dahiya, and N. Abbas, "Cost effective cooling of photovoltaic modules to improve efficiency," *Case Stud. Therm. Eng.*, vol. 14, no. January, p. 100420, 2019, doi: 10.1016/j.csite.2019.100420.

[11] A. A. Sagade, S. K. Samdarshi, P. J. Lahkar, and N. A. Sagade, "Experimental determination of the thermal performance of a solar box cooker with a modified cooking pot," *Renew. Energy*, vol. 150, pp. 1001–1009, 2020, doi: 10.1016/j.renene.2019.11.114.

[12] B. Dalai and M. K. Laha, *Large Eddy Simulation Modeling in 2D Lid-Driven Cavity*, vol. 29. 2021. doi:

10.1007/978-981-15-7831-1_1.

[13] M. H. Sinks *et al.*, "Solar Photovoltaic Panels with Finned Phase Change," 2020.

[14] A. Hasan, S. J. McCormack, M. J. Huang, and B. Norton, "Energy and cost saving of a photovoltaic-phase change materials (PV-PCM) System through temperature regulation and performance enhancement of photovoltaics," *Energies*, vol. 7, no. 3, pp. 1318–1331, 2014, doi: 10.3390/en7031318.

[15] M. A. Sheik *et al.*, "A comprehensive review on recent advancements in cooling of solar photovoltaic systems using phase change materials," no. May 2022, pp. 768–783.

[16] H. Gürbüz, S. Demirtürk, H. Akçay, and Ü. Topalcı, "Thermal stabilization and energy harvesting in a solar PV/T-PCM-TEG hybrid system: A case study on the design of system components," *Energy Convers. Manag.*, vol. 294, p. 117536, Oct. 2023, doi: 10.1016/J.ENCONMAN.2023.117536.

[17] A. B. Awan, "Solar photovoltaics thermal management by employment of microchannels : A comprehensive review," *Int. J. Thermofluids*, vol. 20, no. November, p. 100517, 2023, doi: 10.1016/j.ijft.2023.100517.

[18] N. Abdollahi and M. Rahimi, "Potential of water natural circulation coupled with nano-enhanced PCM for PV module cooling," *Renew. Energy*, vol. 147, pp. 302–309, 2020, doi: 10.1016/j.renene.2019.09.002.

[19] E. Bonah, S. Praveenkumar, N. T. Alwan, V. Ivanovich, and S. E. Shcheklein, "Heliyon Effect of dual surface cooling of solar photovoltaic panel on the ef fi ciency of the module : experimental investigation," *Heliyon*, vol. 7, no. July, p. e07920, 2021, doi: 10.1016/j.heliyon.2021.e07920.

[20] A. Waqas and J. Jie, "Effectiveness of Phase Change Material for Cooling of Photovoltaic Panel for Hot Climate," *J. Sol. Energy Eng. Trans. ASME*, vol. 140, no. 4, pp. 1–19, 2018, doi: 10.1115/1.4039550.

[21] V. Karthikeyan, C. Sirisamphanwong, S. Sukchai, and S. Kumar, "Reducing PV module temperature with radiation based PV module incorporating composite phase change material," *J. Energy Storage*, vol. 29, no. November 2019, p. 101346, 2020, doi: 10.1016/j.est.2020.101346.

[22] K. Velmurugan, S. Kumarasamy, T. Wongwuttanasatian, and V. Seithtanabutara, "Review of PCM types and suggestions for an applicable cascaded PCM for passive PV module cooling under tropical climate conditions," *J. Clean. Prod.*, vol. 293, p. 126065, 2021, doi: 10.1016/j.jclepro.2021.126065.

[23] H. GÜRBÜZ and D. ATEŞ, "A numerical study on processes of charge and discharge of latent heat energy storage system using RT27 paraffin wax for exhaust waste heat recovery in a SI engine," *Int. J. Automot. Sci. Technol.*, vol. 4, no. 4, pp. 314–327, 2020, doi: 10.30939/ijastech..800856.

[24] H. Caliskan, H. Gurbuz, Y. Sohret, and D. Ates, "Thermal analysis and assessment of phase change material utilization for heating applications in buildings: A modelling," *J. Energy Storage*, vol. 50, p. 104593, 2022, doi: https://doi.org/10.1016/j.est.2022.104593.

[25] H. GÜRBÜZ, D. ATEŞ, and H. AKÇAY, "A novel design of heating system using phase change material for passenger car cabin in cold starting conditions," *Int. J. Automot. Eng. Technol.*, vol. 12, no. 3, pp. 92–104, 2023, doi: 10.18245/ijaet.1273428.

[26] N. Abdollahi and M. Rahimi, "Heat transfer enhancement in a hybrid PV/PCM based cooling tower using Boehmite nanofluid," *Heat Mass Transf. und Stoffuebertragung*, 2019, doi: 10.1007/s00231-019-02754-3.

[27] E. B. Agyekum, S. Praveenkumar, N. T. Alwan, V. I. Velkin, S. E. Shcheklein, and S. J. Yaqoob, "Experimental Investigation of the Effect of a Combination of Active and Passive Cooling Mechanism on the Thermal Characteristics and Efficiency of Solar PV Module," 2021.

[28] M. Firoozzadeh, A. H. Shiravi, and M. Shafiee, "Thermodynamics assessment on cooling photovoltaic modules by phase change materials (PCMs) in critical operating temperature," *J. Therm. Anal. Calorim.*, vol. 144, no. 4, pp. 1239–1251, 2021, doi: 10.1007/s10973-020-09565-3.

[29] M. A. Mohammed, B. M. Ali, K. F. Yassin, O. M. Ali, and O. R. Alomar, "Comparative study of different phase change materials on the thermal performance of photovoltaic cells in Iraq's climate conditions," *Energy Reports*, vol. 11, no. November 2023, pp. 18–27, 2024, doi: 10.1016/j.egyr.2023.11.022.

[30] M. Arslan *et al.*, "The effect of using hybrid phase change materials on thermal management of photovoltaic panels – An experimental study," *Sol. Energy*, vol. 209, no. November 2018, pp. 415–423, 2020, doi: 10.1016/j.solener.2020.09.027.

[31] J. Duan, "A novel heat sink for cooling concentrator photovoltaic system using PCM-porous system," *Appl. Therm. Eng.*, vol. 186, no. November 2020, p. 116522, 2021, doi: 10.1016/j.applthermaleng.2020.116522.

[32] S. R. M. Baygi and S. M. Sadrameli, "Thermal management of photovoltaic solar cells using polyethylene glycol 1000 (PEG1000) as a phase change material," *Therm. Sci. Eng. Prog.*, vol. 5, no. May 2017, pp. 405–411, 2018, doi: 10.1016/j.tsep.2018.01.012.

[33] A. Al Miaari and H. M. Ali, "Technical method in passive cooling for photovoltaic panels using phase change material," *Case Stud. Therm. Eng.*, vol. 49, no. July, p. 103283, 2023, doi: 10.1016/j.csite.2023.103283.

[34] A. Ejaz, F. Jamil, and H. M. Ali, "A novel thermal regulation of photovoltaic panels through phase change materials with metallic foam-based system and a concise comparison: An experimental study," *Sustain. Energy Technol. Assessments*, vol. 49, p. 101726, Feb. 2022, doi: 10.1016/J.SETA.2021.101726.

[35] E. B. Agyekum, S. PraveenKumar, N. T. Alwan, V. I. Velkin, and S. E. Shcheklein, "Effect of dual surface cooling of solar photovoltaic panel on the efficiency of the module: experimental investigation," *Heliyon*, vol. 7, no. 9, p. e07920, 2021, doi: 10.1016/j.heliyon.2021.e07920.

[36] F. Jamil *et al.*, "Evaluation of photovoltaic panels using different nano phase change material and a concise comparison : An experimental study," vol. 169, 2021, doi: 10.1016/j.renene.2021.01.089.

[37] L. Siahkamari, M. Rahimi, N. Azimi, and M. Banibayat, "Experimental investigation on using a novel phase change material (PCM) in micro structure photovoltaic cooling system," *Int. Commun. Heat Mass Transf.*, vol. 100, pp. 60–66, 2019, doi: 10.1016/j.icheatmasstransfer.2018.12.020.